The EMBO Journal Vol.17 No.24 pp.7282–7293, 1998

A function–structure model for NGF-activated TRK

Matthew E.Cunningham and Lloyd A.Greene[1]

Department of Pathology and Center for Neurobiology and Behavior, College of Physicians and Surgeons, Columbia University, New York, NY 10032, USA

[1]Corresponding author
e-mail: LAG3@Columbia.edu

Mechanisms regulating transit of receptor tyrosine kinases (RTKs) from inactive to active states are incompletely described, but require autophosphorylation of tyrosine(s) within a kinase domain 'activation loop'. Here, we employ functional biological assays with mutated TRK receptors to assess a 'switch' model for RTK activation. In this model: (i) ligand binding stimulates activation loop tyrosine phosphorylation; (ii) these phosphotyrosines form specific charge pairs with nearby basic residues; and (iii) the charge pairs stabilize a functionally active conformation in which the activation loop is restrained from blocking access to the kinase catalytic core. Our findings both support this model and identify residues that form specific charge pairs with each of the three TRK activation loop phosphotyrosines.

Keywords: conformation/electrostatic/phosphorylation/RTK/tyrosine

Introduction

Intensive research over the past several decades has revealed that receptor tyrosine kinases (RTKs) respond to ligand occupancy through sequential steps of oligo- or dimerization, rapid autophosphorylation of the 1–3 tyrosine residues that lie within the 'activation loop' of the kinase domain, full activation of the kinase, continued autophosphorylation at sites outside of the kinase domain and, finally, association with and phosphorylation of intracellular targets that propagate the signal (Ullrich and Schlessinger, 1990; Schlessinger and Ullrich, 1992; McDonald *et al*., 1995). A key question about this process is how occupancy converts receptors from an 'off' state to a fully functional active state. Structure–function studies with a variety of RTKs indicate that ligand-stimulated autophosphorylation of kinase domain 'activation loop' tyrosines is an early obligatory step in ligand-mediated kinase activation (Rosen *et al*., 1983; Herrera and Rosen, 1986; Tornqvist and Avruch, 1988; White *et al*., 1988; Li *et al*., 1994; Longati *et al*., 1994; Hernández-Sánchez *et al*., 1995; McCarty and Feinstein, 1998). However, the molecular mechanisms by which such autophosphorylation leads to receptor activation are only beginning to be understood. A crystallographic study of the non-phosphorylated insulin receptor kinase domain (IRK) indicated that in this state, the activation loop Tyr1162 acts as a pseudosubstrate that blocks access of substrate tyrosines and of ATP to the catalytic core (Hubbard *et al*., 1994). It was suggested, in accord with previous reports of conformational changes in insulin receptor activation (Baron *et al*., 1992; Kaliman *et al*., 1993; reviewed in Van Obberghen *et al*., 1993) that ligand-stimulated autophosphorylation of activation loop tyrosines results in loss of this inhibitory interaction which, in turn, promotes maximal kinase activation.

We have utilized the TRK receptor of nerve growth factor (NGF) as a model for RTK activation. In a neuronal environment, TRK mediates NGF responses including long- and short-term gene regulation, neuronal differentiation and survival in serum-free medium (reviewed in Greene, 1984; Green *et al*., 1986; Loeb *et al*., 1991; Loeb and Greene, 1993; Greene *et al*., 1998). *In vitro* assessment has identified TRK tyrosine residues 490, 670, 674, 675 and 785 as autophosphorylation sites (Stephens *et al*., 1994). The first and last of these are required for binding and tyrosine phosphorylation of signaling molecules such as Shc and phospholipase Cγ-1 (PLCγ-1) (Loeb *et al*., 1994; Stephens *et al*., 1994); the other three tyrosines lie within the kinase activation loop and are involved in TRK activation (Segal *et al*., 1996; Cunningham *et al*., 1997). In a biologically based study of TRK activation loop tyrosines, we found that mutation of either Tyr670, Tyr674 or Tyr675 significantly impairs NGF-inducible responses including promotion of neurite outgrowth and tyrosine phosphorylation of Shc/ERKs and of PLCγ-1 (Cunningham *et al*., 1997). Although neuritogenic capacity and Shc/ERK signaling were substantially rescued by high overexpression of mutant receptors, loss of PLCγ-1 phosphorylation was not. The latter correlated with loss of TRK autophosphorylation at its C-terminal binding site for PLCγ-1, Tyr785. The observation that all three activation loop tyrosines participate in TRK activation led us to suggest that ligand binding and consequent phosphorylation of activation loop tyrosines leads not only to removal of an inhibitory interaction, but also to stabilization of the TRK intracellular domain in a conformation that promotes kinase activity and ability to access Tyr785. We further hypothesized that this functionally active conformation would be stabilized, at least in part, by creation of charge pairs between the activation loop phosphotyrosines and nearby positively charged residues. Our hypothesis is supported by a recent crystallographic study of activated IRK which indicated that two of the three phosphorylated activation loop tyrosines each interacts pairwise with basically charged residues, and that activation is accompanied by a large conformational change (Hubbard, 1997).

The purposes of the present study were several-fold. The first was to devise a suitable biological test for the

concept that charge pairs formed between phosphorylated activation loop tyrosines and nearby positively charged residues are required for ligand-mediated functional activation of RTKs. The second was, for the case of the TRK receptor, to identify the residues involved in such interactions. We also sought to exploit our biological screens of function to identify additional charged residues that might be important for stabilizing the active TRK conformation.

Results

Functional bioassays for TRK activation loop mutants

To study the role of the TRK activation loop tyrosines in receptor function, we mutated these sites (Tyr670, Tyr674 and Tyr675), individually and in all combinations, to phenylalanines and inserted the wild-type and mutant TRKs into recombinant retroviruses. The latter were used to infect PC12nnr5 cells which lack endogenous TRK. Polyclonal cultures of infected cells were generated and assessed for NGF-promoted neuritogenesis. Results were similar to our previous report of NGF-induced neuritogenesis in multiple clonally derived PC12nnr5 lines with varying levels of wild-type and mutant receptor expression (Cunningham *et al*., 1997); singly mutated receptors Y670F and Y674F retained the highest residual function, and the Y675F mutant and all double combination mutants exhibited little or no neuritogenic activity (Figure 1A). This behavior of the polyclonal cultures is similar to that of clonal lines expressing the respective TRKs at levels at least 20-fold that found in PC12 cells (Cunningham *et al*., 1997). Western immunoblotting confirmed this level of expression in the polyclonal cultures (not shown).

To extend and complement the neuritogenic assay, we also delivered the wild-type and mutant TRKs into NIH 3T3 cells. Fibroblasts transfected with TRK (Cordon-Cardo *et al*., 1991) respond to NGF by transformation, focus formation and anchorage-independent growth. The infected NIH 3T3 cells were subcultured and subjected to either G418 selection (100 μg/ml), no treatment or NGF stimulation (150 ng/ml). Cultures infected with wild-type TRK and maintained for 4–7 days past confluence developed NGF-dependent populations of transformed colonies that were much more rounded and phase-bright than the background cells and that were easily detected in dark field illumination by their distinctive refractiveness (not shown). The transformed cells also showed TRK immunoreactivity (not shown). No transformed colonies were detected without NGF. Transformation efficiency with virus expressing wild-type TRK was 68 ± 10% (n = 12) (Figure 1B) as defined by the ratio of the total number of NGF-induced transformed colonies observed to the total number of virions delivered (see Materials and methods). Functional activities of the mutant receptors in this assay (Figure 1B) were identical to those achieved with the polyclonal PC12nnr5 cells (Figure 1A); the Y670F and Y674F mutants showed strong transformation activity while the Y675F mutant and all double combination mutants were only weakly active, as was the K538N kinase-deficient TRK. Taken together, these observations indicate that mass cultures of transfected NIH 3T3 and PC12nnr5 cells are suitable to bioassay the relative functional activities of TRK mutants.

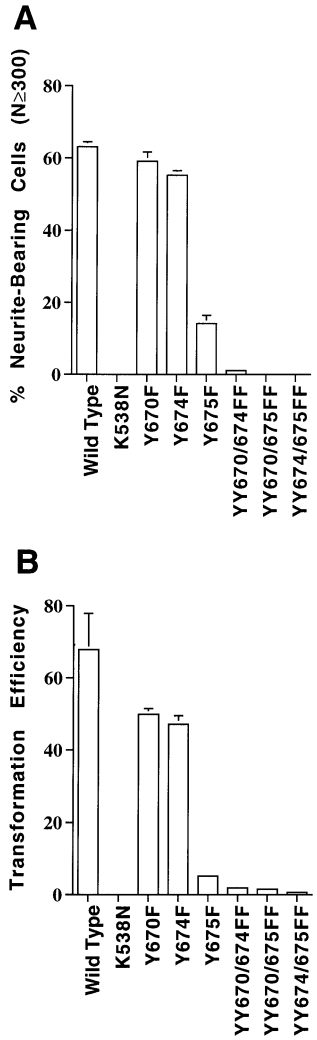

Fig. 1. NGF-promoted mediation of NIH 3T3 cell transformation and polyclonal PC12nnr5 cell differentiation by wild-type and activation loop tyrosine mutant TRKs. (**A**) PC12nnr5 cells were stably transfected with the indicated TRKs, were grown as polyclonal cultures and were assessed for NGF-induced neuritogenesis. Reported values were assessed at day 7 of NGF treatment and are averages ± SEM. Comparable results were obtained in a duplicate experiment. (**B**) Recombinant LNC retroviruses containing wild-type or the indicated mutant TRKs were used to infect NIH 3T3 'N' cells which were expanded and subjected to NGF, G418 or no treatment as described in Materials and methods. After 7–10 days of treatment, transformed colonies of cells were apparent under low magnification phase-contrast microscopy. Transformation and viral titers were assessed under dark field microscopy, and efficiencies were calculated as described in Materials and methods. Reported values are averages ± SEM from triplicate, independent experiments. No transformation was observed in the absence of NGF here or in subsequent experiments.

A functional screen for contacts of phosphorylated activation loop tyrosines

Our prior findings indicated that mutation of any of the activation loop tyrosines leads to diminished TRK function (Cunningham *et al*., 1997). Also indicated in that study, and confirmed here, was that this impairment can be rescued by overexpression in the cases of Y670F and Y674F, but not for Y675F or any double combination

mutation of these sites. We suggested that one mechanism to explain the role of these tyrosines is that after phosphorylation they interact with nearby charged (or polar) residues and that such contacts in turn contribute to formation and stabilization of a fully activated TRK conformation. Disruption of any of the phosphorylations would impair such interactions, destabilize the activated conformation and consequently diminish receptor function. We further reasoned that if such interactions occur, then function should be equally affected by mutation of the corresponding charge partner of an activation loop phosphotyrosine. Employing these points, we developed a strategy to test our model and to identify charge partners for each of the activation loop phosphotyrosines. In this screen, candidate charge pair partners were mutated to alanine and evaluated for function (NGF-dependent transformation and/or neurite outgrowth) in backgrounds in which none (wild-type) or each of the activation loop tyrosines were mutated individually to phenylalanine. As an example (Figure 2A), a TRK bearing a mutation at either Tyr670, the charge partner for Tyr670, or both of these sites would show little loss of function when overexpressed. The same is true for Tyr674 and its corresponding charge partner. In contrast, when TRKs with paired mutations of Y670F and the charge partner for Tyr674, or of Y674F and the charge partner for Tyr670 are overexpressed, function would be expected to be lost because the YY670/674FF double mutation would be simulated (Figure 2A). These concepts allow a definition to be made of the phosphotyrosine charge pair partner that is grounded in preserved background-specific function. Namely, a charge pair partner candidate, when mutated alone, must have NGF-inducible function comparable with that of the singly mutated activation loop tyrosines (Y670F or Y674F), and must retain a similar level of inducible function in one of the backgrounds of mutant activation loop tyrosines while losing function in the other two. The specific phosphotyrosine involved in charge pairing with the candidate residue is then the background in which function is preserved. Initially, a potential limitation of our proposed screen was that the Y675F mutation alone shows little activity and therefore might not show further functional loss when paired with additional mutations.

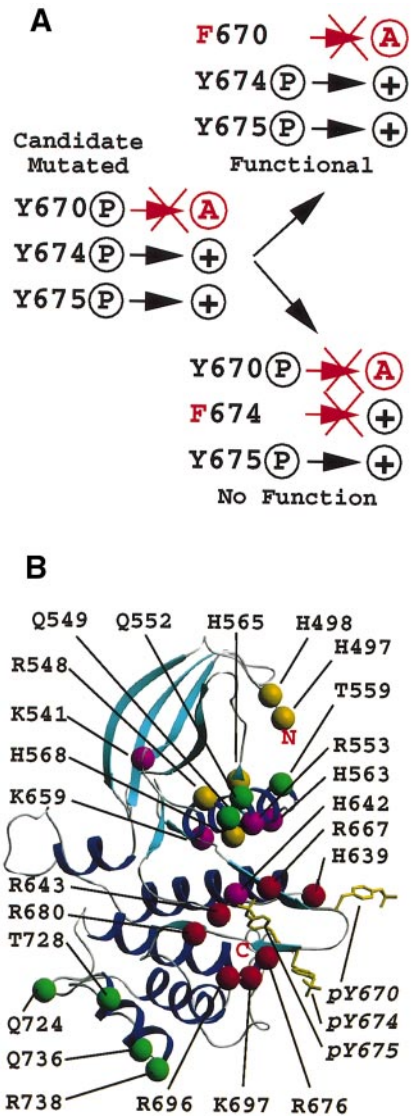

Fig. 2. Rationale for functional screen-in-backgrounds and model for candidate residue locales. (**A**) NGF-induced TRK function requires two fully intact phosphotyrosine-based bridging interactions. Disruptions of a candidate charge, or of this and its phosphotyrosine partner retain function (left and upper situations), but disruptions involving two bridges result in loss of function (bottom). (**B**) Structural coordinates from the active IRK crystal structure (Brookhaven PDB, accession No. 1IR3) were adapted to depict graphically the candidate polar and basic TRK residues evaluated in this study using SETOR (Evans, 1993). TRK residues are identified on the structure as deduced by comparison of the primary sequences of the kinase domains. Mutant sites are color coded as follows: yellow indicates constructs that were not expressible, magenta indicates loss of function mutants, green indicates neutral mutations and red indicates background-specific function as predicted by our model.

Identification of charge pair partners for phosphotyrosines 670 and 674

To implement the above screen, candidate residues for mutation were chosen on the basis of their positive charge or polar character, and of their potential three-dimensional positions relative to the activation loop tyrosines as predicted by imposition of the homologous TRK sequence on the crystal structures of the insulin and fibroblast growth factor (FGF) receptor kinase domains (Hubbard *et al*., 1994; Mohammadi *et al*., 1996; Hubbard, 1997). Comparison of the primary sequence of TRK (amino acids 486–790) with the construct used for crystallizing IRK (Hubbard *et al*., 1994) demonstrated 44% identity and 61% homology between the proteins. To aid the interpretation of the findings presented here, Figure 2B shows the TRK sites evaluated in this study superimposed onto the crystal structure of the activated IRK (Hubbard, 1997), which are color coded as defined in the legend. Because of the large number of candidate residues to be assessed, initial studies were carried out with the NIH 3T3 cell transformation assay.

Several of the mutations, Q552A (Figure 3A), Q549A and T559A (data not shown), had no effect on function in all four backgrounds (wild type, Y670F, Y674F or Y675F) (compare Figures 1B and 3A). Likewise, preliminary findings showed that mutation of Gln724, Thr728, Gln736 or Arg738 did not affect TRK function in the Y674F background (data not shown). This indicates that mutations of nearby charged or polar residues do not lead indiscriminately to loss of activity. In contrast, TRKs

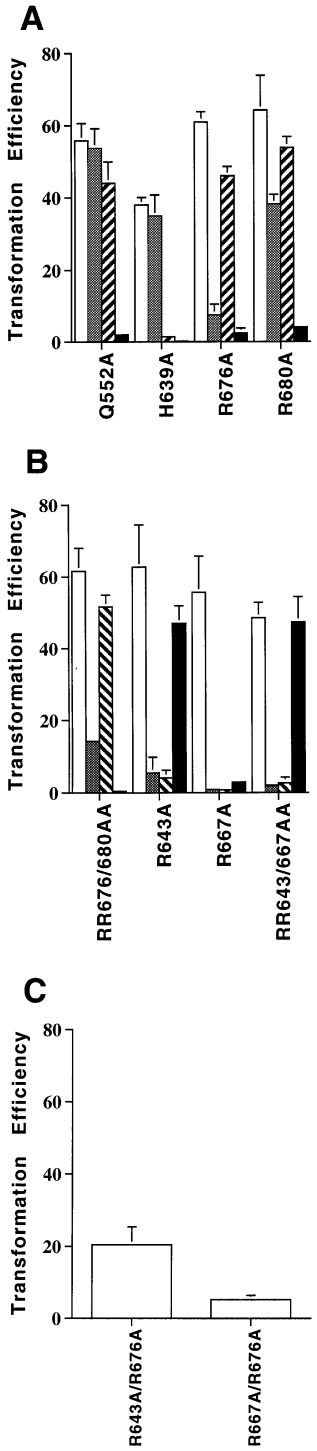

Fig. 3. Mutation of Gln552 does not impair NGF-inducible TRK function, and His639 and arginines 643, 667, 676 and 680 form functional charge pairs with phosphorylated activation loop tyrosines. NIH 3T3 cells were infected with recombinant retroviruses bearing the indicated TRKs, expanded and subjected to NGF, G418 or no treatment as described in Materials and methods. Values reported are the averages ± SEM of three independent experiments. (**A** and **B**) Receptor mutants bearing mutations of the indicated positively charged residues in the backgrounds of wild-type (filled white) or with each of the activation loop tyrosines mutated individually (Y670F filled gray, Y674F cross-hatched and Y675F filled black). (**C**) Receptor mutants bearing the R643A/R676A and R667A/R676A double mutations in the background of wild-type activation loop tyrosines.

bearing mutations at Lys541 or His642 showed loss of function in all backgrounds. The latter point mutant lost the capacity to become tyrosine autophosphorylated in response to NGF (data not shown), indicating that His642 plays an indispensable role in TRK kinase function. The corresponding IRK residue (His1130) was reported to form main chain interactions that stabilize the catalytic loop (Hubbard *et al*., 1994). Interestingly, despite the loss of NGF-inducible biological activity, the K541A point mutant retained a significant level of NGF-dependent autophosphorylation (data not shown). Substitution of the TRK residues Glu512 and Lys541 in the IRK activated structure reveals the potential for interaction of these two sites. Thus, the mechanism for impairment of the Lys541 mutant may involve disruption of a standing electrostatic interaction that in turn leads to disordering of the activated state. Three other candidates, Arg553, His563 and Lys659, showed significantly diminished function in the wild-type background (each with 21–25% transformation efficiency) and showed little to no function in the other backgrounds. Because none of these mutants fulfill the criteria for a phosphotyrosine charge pair partner, they were not investigated further in this study. Mutation of several other potential interaction sites resulted in loss of expression and thus their potential contributions as phosphotyrosine interactors could not be assessed. As inferred from the IRK crystal structure, these poorly expressible mutants either precede the kinase domain (His497 and His498), are contained in α-helix C (Arg548) or are located in the interdomain hinge region of the kinase (His565 and His568) (Figure 2B).

Several mutations of positively charged residues exhibited background-specific effects on function that conformed to the predictions of our model (Figure 3). The H639A mutation showed significant activity in the wild-type and Y670F backgrounds and little to no activity in the Y674F or Y675F backgrounds (Figure 3A). Although the absence of activity in the Y675F background is not informative, as described above, the loss of activity in the Y674F background identifies His639 as a charge partner for phosphotyrosine 670 (pY670). Similarly, the R676A mutation is active in the wild-type and Y674F backgrounds, but not when combined with the Y670F or Y675F mutations (Figure 3A) and, therefore, this arginine behaves as a functional charge pair partner for pY674. Likewise, the R680A mutation exhibited a partial, but significant ($p = 0.1$, by Student's *t*-test) diminution of activity in the Y670F background when compared with the wild-type background, and preserved activity in the Y674F background (Figure 3A); this suggests that this residue may be a weak charge pair partner for pY674. Consistent with this, the functional activity of the combined RR676/680AA mutations assessed in the four test backgrounds showed no further loss when compared with that of the R676A mutation alone (compare Figure 3A with B).

Mutation of Arg643 restores the activity of Y675F and permits the identification of arginines 643 and 667 as charge pair partners for pY675

Unexpectedly, mutation of Arg643 selectively restored function in the Y675F background so that the R643A/Y675F double mutant was as functional in the transforma-

tion assay as the Y670F and Y674F single mutants (compare Figures 1B and 3B). In contrast, the R643A/Y670F and R643A/Y674F double mutants showed nearly total loss of activity, while the R643A mutation in the wild-type background caused no loss of activity. These observations suggest several points. First, rescue by the R643A mutation is not simply a result of general activation since it was background specific, and since, irrespective of the background, receptors with this mutation failed to show activity without NGF (data not shown). Secondly, R643A follows the pattern of function predicted by our model, with specific loss of function in the Y670F and Y674F backgrounds, and thus Arg643 appears to be a charge pair partner for pY675. Thirdly, these findings suggest a mechanism for the dramatic loss of function in the Y675F single mutant as compared with the Y670F or Y674F single mutants: in the absence of pY675, another charged residue (perhaps pY674) may interact inappropriately with Arg643. This interpretation would explain why the R643A mutation restores function in the Y675F background. When Arg643 is mutated, the incorrect charge pair cannot form and the phenotype would be equivalent to the loss of only a single charge pair interaction (i.e. like Y670F or Y674F).

The observation that the R643A mutation rescues Y675F function permitted us to seek additional partners for phosphorylated Tyr675. Our initial screen revealed that the R667A mutant TRK possesses efficient NGF-induced transformation activity in the wild-type background, but little or no activity when combined with any of the three mutant activation loop tyrosines (Figure 3B). The loss of activity in the Y670F and Y674F backgrounds is consistent with the possibilities that Arg667 is a charge pair partner for pY675 and that, unlike R643A, mutation of Arg667 does not restore function to the Y675F background. Support for these possibilities is provided by the crystal structure of the activated LCK kinase domain which indicates charge pairing homologous to both the R643–pY675 and R667–pY675 TRK interactions. To test this hypothesis, the double TRK mutant RR643/667AA was prepared and assessed in all four backgrounds. The rationale was that if Arg667 were a charge pair partner for pY675, combination with the R643A mutation would rescue function selectively in the Y675F background, but not the Y670F or Y674F backgrounds. As shown in Figure 3B, this is the case, thus indicating that Arg667 and Arg643 are both charge partners for pY675. When this strategy was applied to additional candidates, Gln724, Thr728, Gln736 and Arg738 were excluded as partners for pY675 as were Arg676 and Arg680 (data not shown).

Combination mutants of charge pair partners

An important prediction of our model is that combined mutation of charge pair partners for different phosphotyrosines should lead to the same loss of function seen with combined mutation of the phosphotyrosines themselves. To test this, combined mutations of pY674 and pY675 charge pair partners were assessed in a background of wild-type phosphotyrosines (Figure 3C). In agreement with the model, the R676A/R667A combination showed nearly total loss of function. The R643A/R676A mutant also lost significant, but not total, function. The partial function remaining in this mutant suggests a partial stabilizing influence by the remaining pY675 interactor, Arg667. Similarly, in accordance with its weak putative interaction with pY674, paired mutation of Arg680 with pY675 interactors showed little loss of function (data not shown).

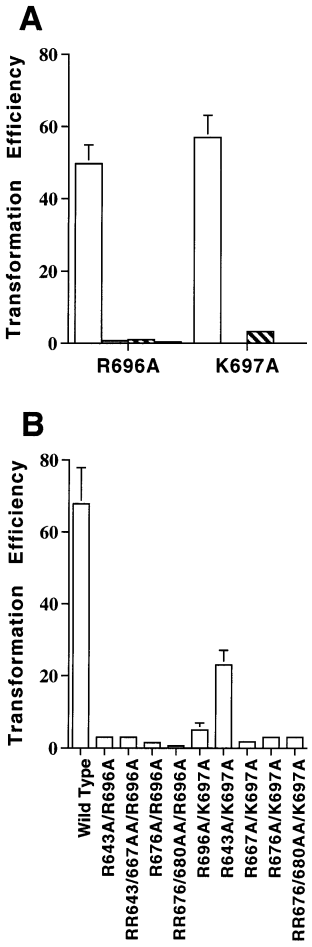

Fig. 4. Arg696 and Lys697 do not interact with activation loop phosphotyrosines, but stabilize NGF-activated TRK. NIH 3T3 cells were infected with recombinant retroviruses bearing the indicated TRKs, expanded and subjected to NGF, G418 or no treatment, as described in Materials and methods. Values reported are the averages ± SEM of three independent experiments. (**A**) Receptor mutants bearing mutations of the indicated positively charged residues in the backgrounds of wild-type (filled white) or with each of the activation loop tyrosines mutated individually (Y670F filled gray, Y674F cross-hatched and Y675F filled black). (**B**) Receptor mutants bearing the indicated combination mutations in the background of wild-type activation loop tyrosines.

Arg696 and Lys697 play roles in stabilization of activated TRK, but do not appear to be charge pair partners for activation loop phosphotyrosines

Two additional mutations of charged residues (R696A and K697A) were identified that, like R667A, resulted in loss of NGF-dependent function in all three backgrounds of activation loop mutations, but not in the wild-type background (Figure 4A). These observations seem to rule out interactions with pY670 and pY674 but, as discussed for the R667A mutation, do not rule out interaction with pY675. To assess these possibilities further, combination mutations of charge pair partners (Arg643, Arg667, Arg676 or Arg680) with R696A or K697A were evaluated for function in the background of wild-type activation loop

tyrosines (Figure 4B). The RR676/696AA and R676A/K697A mutant TRKs were not functional, confirming that Arg696 and Lys697 do not interact with pY674. Furthermore, all mutant TRK combinations containing R696A or K697A and charge pair partners for pY675 were highly to totally impaired, which eliminates the possibility that either Arg696 or Lys697 interacts with pY675. In addition, when R643A was superposed onto the R696A/Y675F mutant, function in this background was not rescued (transformation efficiency 2.4%). The partial activity retained by the R643A/K697A receptor is similar to that of the RR643/676AA receptor, and thus probably reflects the stabilizing influence of the remaining pY675 interactor, Arg667. Taken together, these observations indicate that Arg696 and Lys697 help to stabilize the TRK active state, but do so by a mechanism other than by interaction with activation loop phosphotyrosines. Another interesting point here is the functional loss shown in the R696A/K697A double mutant receptor (Figure 4B), which indicates that either the two residues act independently or that they interact with a common site that is tolerant to loss of one, but not both interactions.

Assessment of function in the PC12nnr5 cell neurite outgrowth assay confirms assignment of charge pair partners

To determine if the above findings are applicable to a neuronal environment (which is more typical for TRK expression and function), selected mutant TRKs from the preceding experiments were assessed in the PC12nnr5 cell neurite outgrowth rescue assay (Loeb *et al*., 1991). Comparison of results from the neurite outgrowth assay (Figure 5) with those obtained in the transformation assay (Figure 3) revealed nearly identical findings, which confirmed that mutation of Gln552 has no evident phenotype in any background, and that His639, Arg676 and Arg643 are charge pair partners for pY670, pY674 and pY675, respectively. The parallel degrees of function observed in both assays suggest that the levels of biological 'readout' in each system (i.e. mitogenesis or differentiation) is dependent more upon the functional capacity of the mutant TRK receptor than upon its cellular context.

Mutation of charge pair partners for activation loop phosphotyrosines selectively impairs NGF-dependent phosphorylation of PLCγ-1

In our study of clonal PC12nnr5 cells, mutation of any one of the TRK activation loop tyrosines resulted in selective, severe impairment of NGF-dependent PLCγ-1 tyrosine phosphorylation, even when the receptors were highly overexpressed (Cunningham *et al*., 1997). This appeared to be due to loss of the capacity of the mutated receptors to autophosphorylate the PLCγ-1-binding site, Tyr785. In contrast, the extent of Shc phosphorylation was diminished, but, in parallel with biological function, was substantially rescued by receptor overexpression. We interpreted these findings to suggest that phosphorylation of activation loop tyrosines not only regulates TRK activation, but also contributes to stabilization of a conformational change that permits phosphorylation of Tyr785. If our charge pair model is correct, then mutation of phosphotyrosine charge pair partners should also selectively compromise NGF-promoted PLCγ-1 phosphorylation. When this was assessed in polyclonal PC12nnr5 cell cultures, the results were in accord with this prediction (Figure 6). That is, single mutations of His639, Arg676 or Arg667, which we identified as 'strong' charge partners for pY670, pY674 and pY675 respectively, led to greatly diminished PLCγ-1 tyrosine phosphorylation (Figure 6A). These effects were both specific and selective. Each of the mutant receptors retained the capacity to stimulate substantial levels of Shc phosphorylation (Figure 6B), TRK autophosphorylation (data not shown) and, as demonstrated above, to mediate biological function (neurite outgrowth, Figure 5). In contrast, mutation of Arg680, a weak interactor for pY674, had little effect on PLCγ-1 tyrosine phosphorylation. Likewise, mutation of the pY675 interactor Arg643, which, based on functional studies in various TRK mutant backgrounds (Figures 3C and 4B), appears to have only a partial destabilizing effect on the activation loop, yielded a partial reduction in PLCγ-1 phosphorylation.

NGF-dependent PLCγ-1 and Shc phosphorylation were also assessed in the R696A and K697A mutants. Here again, PLCγ-1 phosphorylation was severely depressed

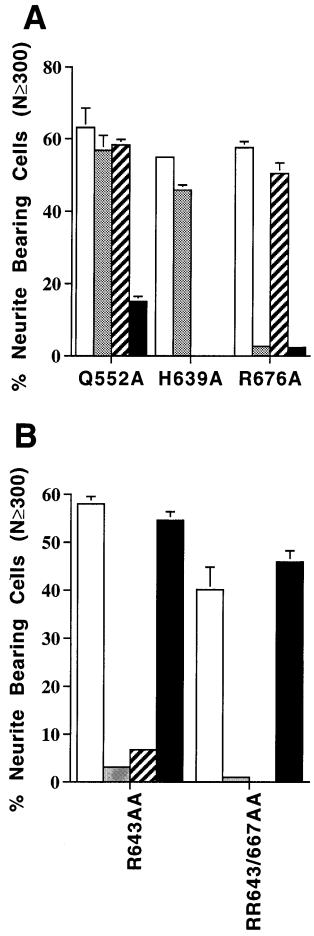

Fig. 5. Neuritogenic activity of TRKs bearing mutations of identified charge pair partners. Polyclonal cultures of PC12nnr5 cells stably transfected with the indicated TRKs were assessed for NGF-induced neuritogenesis at a 7 day time point. TRKs contain mutations of positively charged residues in backgrounds of wild-type (filled white) or with each of the activation loop tyrosines mutated individually (Y670F filled gray, Y674F cross-hatched and Y675F filled black). Reported values are the averages ± SEM for a representative, duplicated experiment.

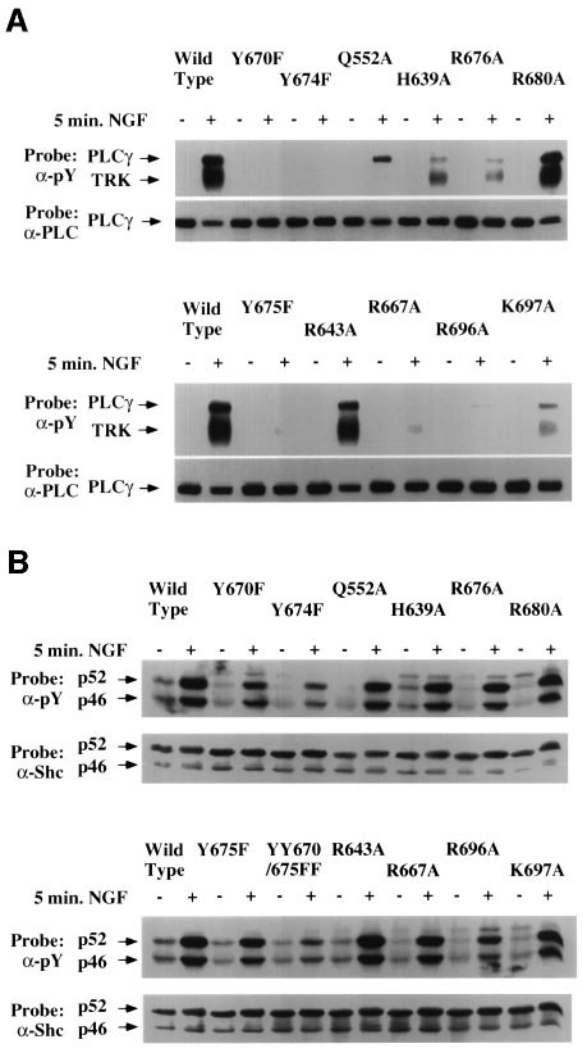

Fig. 6. Mediation of NGF-induced tyrosine phosphorylation of Shc and PLCγ-1 by charge pair partner mutant TRKs in transfected PC12nnr5 cells. Detergent-solubilized cell lysates (containing 3 mg of protein) from the indicated NGF-treated and control cells expressing the indicated wild-type and mutant TRKs were subjected to immunoprecipitation with anti-PLCγ-1 (**A**) or anti-Shc (**B**) as described in Materials and methods. The immunoprecipitates were subjected to Western immunoblotting and were serially probed with anti-phosphotyrosine (4G10) and anti-idiotype antibodies.

whereas Shc phosphorylation was largely intact (Figure 6). In agreement with the selective effect on PLCγ-1, substantially preserved neuritogenic responses were observed for the R696A and K697A TRK-expressing cell lines (49 ± 4% and 57 ± 4%, respectively). Taken together, these observations indicate that contacts between activation loop phosphotyrosines and their charge pair partners as well as between Arg696 and Lys697 and their non-phosphotyrosine contacts stabilize a conformation that is required for autophosphorylation of TRK Tyr785.

Discussion

The present study was undertaken to address how ligand-dependent autophosphorylation of activation loop tyrosines leads to functional activation of RTKs. In particular, we evaluated the model that: (i) in the non-phosphorylated state, the activation loop occludes access of ATP and substrates to the catalytic core of the receptor; (ii) the phosphotyrosines generated by autophosphorylation form charge pairs with nearby basic residues; and (iii) these interactions help stabilize a fully functional active conformation with full access to the catalytic core. We also sought to determine the identities of the interacting basic residues in the TRK NGF receptor and thereby to provide a representation of how the activation loop is situated in the activated state. To achieve this, we devised biologically based functional assays predicated on the ideas that each of the activation loop tyrosines interacts with distinct charged residue(s), that these interactions can be disrupted by mutation of either partner of the charge pair and that disruption of two or more charge pairings (from different phosphotyrosines) results in loss of NGF-inducible biological function.

Ligand-induced mutant TRK function is similar in dissimilar cell backgrounds

Two cell lines were used in our studies: NIH 3T3 cells permitted rapid assessment of mutated TRK function in a transformation assay, whereas PC12nnr5 cells allowed assessment in a more neuronal environment in which the endpoint was NGF-promoted neurite outgrowth. Significantly, there was strong concordance between the results achieved in both systems (Figure 1, and compare Figure 3 with 5). It has been reported that overexpression of activated Ras/ERK pathway constituents drives fibroblast proliferation and PC12 cell neurite outgrowth (Cowley *et al*., 1994). Our past findings indicate that functionally active TRKs retain strong ERK signaling, whereas those without functional activity do not. This suggests that the extent of biological function exhibited by various mutant TRKs in our two cell systems reflects, at least in part, the degree to which the ERK pathway is activated by NGF.

We previously stressed the importance of expression levels in assessing function of mutated TRKs (Cunningham *et al*., 1997). For instance, the Y670F and Y674F mutants mediate robust neurite outgrowth when expressed at 10- to 20-fold the levels of wild-type TRK in PC12 cells, but are significantly impaired below this level of overexpression. Here, we used polyclonal cultures. When we compared results from clonal and polyclonal PC12nnr5 cell cultures, our findings were entirely consistent with one another, and indicated that on average the polyclonal cells responded like clonal cells expressing at least 20-fold the receptor levels of wild-type PC12 cells. This level of overexpression permitted us to detect functional activity in receptors bearing single charge pair mutations and loss of activity in receptors mutated such that two charge pairs are lost.

NGF-activated TRK is stabilized by interactions involving charge pairs with activation loop phosphotyrosines and non-charge pair based contacts

Our functional assays screened a number of residues as potential charge partners for activation loop phosphotyrosines. Findings included residues without apparent effect on TRK function when mutated (Gln549, Gln552, Thr559, Gln724, Thr728, Gln736 and Arg738) as well as residues whose mutation led to complete (Lys541 and His642) or near-complete (Arg553, His563 and Lys659) loss of TRK

function in all backgrounds tested. We also identified residues that, when mutated to alanine, led to loss of function in specific activation loop tyrosine mutant backgrounds, and that therefore fulfilled our criteria as charge pair partners for activation loop phosphotyrosines. These residues include His639 (for pY670), Arg676 and Arg680 (for pY674), and Arg643 and Arg667 (for pY675). We cannot rule out the possibility that the activation loop phosphotyrosines form additional stabilizations either with the peptide backbone, as described in the IRK (Hubbard, 1997), or with other residues not assessed here.

The observation that TRK function can be impaired equally by mutating either partner of a phosphotyrosine–basic residue charge pair suggests that phosphorylation of activation loop tyrosines accomplishes more than simply removing these as potential pseudosubstrates. Rather, our experiments indicate that phosphorylation permits each of the activation loop tyrosines to form specific electrostatic charge pairs with nearby positive charges and that multiple interactions of this type stabilize the receptor in a functionally active state. Our studies highlight the biological importance of each of these electrostatic interactions, in that compromising any one leads to functional impairment.

We identified two positively charged residues (Arg696 and Lys697) that appear to participate in stabilizing the TRK activated state, but which do not associate with activation loop phosphotyrosines. The putative partners for these sites currently are not identified, but inspection of the TRK sequence and comparison with the structure of the activated IRK suggest Asp673 as a potential candidate. Preliminary observations using a biological function-based screen in backgrounds similar to the one used in this study suggest that Asp673 does not interact with Lys697 (data not shown), but we did not assess the potential interaction of Asp673 with Arg696.

Destabilizing actions of the Y675F mutation

Our findings reveal that unlike the Y670F and Y674F mutants, the Y675F mutant lacks biological activity, even when highly overexpressed. An unanticipated observation was that combination of the R643A mutation with Y675F restores function. A potential explanation is that the Y675F mutation permits inappropriate interaction of another acidic residue with Arg643 and that this in turn permits an unfavorable conformation that lacks function. In this model, mutation of Arg643 to a non-charged residue eliminates the inappropriate interaction. This would explain why the R643A/Y675F mutant has functional behavior equivalent to that of the single mutants of Y670F or Y674F. Candidate partners for such an ectopic interaction include pY670 or pY674. If one of these were to interact with Arg643 in the Y675F background, this would be equivalent to perturbation of two activation loop tyrosines and thus, as observed, to loss of function. Alternative candidates for the ectopic acidic charge are Asp673 or a carbonyl group from the activation loop peptide backbone. The potential backbone interaction cannot be disturbed by point mutation and thus cannot be assessed in our system, but when the D673A mutation was combined with Y675F, TRK function was not restored (data not shown).

Activation loop charge pair interactions stabilize a TRK conformation that permits PLCγ-1 phosphorylation

Our past study indicated that TRK-mediated PLCγ-1 phosphorylation is nearly completely compromised by mutations of single activation loop tyrosines, whereas Shc phosphorylation can be rescued substantially by overexpression of the same mutants. Here, we find that receptors with single mutations of activation loop stabilizers (Arg696 and Lys697) or of strong charge pair partners for activation loop phosphotyrosines (His639, Arg676 and Arg667) also severely compromise NGF-dependent PLCγ-1 phosphorylation, but support both biological function and Shc phosphorylation. These observations support our supposition that mutation of either side of a charge pair can be functionally equivalent, and support the hypothesis that interactions formed by the phosphorylated TRK activation loop serve to stabilize the receptor in a conformation that is not only catalytically active, but that is required for interaction with and phosphorylation of substrates at the C-terminus of the receptor. With respect to this latter point, we cannot rule out the alternative possibility that Tyr785 is a relatively poor substrate for TRK and is therefore more sensitive to impairment of kinase activity. However, analysis of TRK autophosphorylation sites indicates that Tyr785 is as good as or better a substrate than Tyr490, the Shc site (Loeb *et al*., 1994).

Inferred structural features of the activation loop in TRK activation

In the present work, we used biologically based functional assays to infer structural features of an activated RTK. This is in some contrast to crystallographic studies that interpret structural data to infer information about function. Thus, comparison of findings from the two approaches are complementary. At present, crystal structures are available for the inactive FGF receptor kinase domain (Mohammadi *et al*., 1996), the activated state of the nonreceptor tyrosine kinase LCK (Yamaguchi and Hendrickson, 1996) and both states of the IRK (Hubbard *et al*., 1994; Hubbard, 1997). Structures of the kinase domains of active and inactive serine/threonine kinases have also been solved (reviewed in Wei *et al*., 1994; Bossemeyer, 1995; Johnson *et al*., 1996) and are exemplified by that of cAMP-dependent kinase (PKA) (Zheng *et al*., 1993).

Overall, the structures have many similarities, as well as differences, with one another and with the structure inferred here for TRK. In the comparisons to follow, homologous residues of TRK will be given in parentheses. Activated PKA (Zheng *et al*., 1993) has a single phosphothreonine, pT197, that is the apparent functional homolog of TRK pY675. The structure (modeled in Hubbard, 1997) indicates interactions of pT197 with His87 of α-helix-C (TRK Asp550), Arg165 (TRK Arg643), Lys189 (TRK Arg667) and Thr195 (TRK Asp673). Activated LCK has a single phosphotyrosine pY394, which is also the apparent homolog of TRK pY675 and which, in apparent homology with TRK pY675, interacts with Arg363 (TRK Arg643) and Arg387 (TRK Arg667). Activated IRK has three activation loop phosphotyrosines that are the direct homologs of those in TRK. The deduced crystal structure indicates interactions of pY1162 (TRK

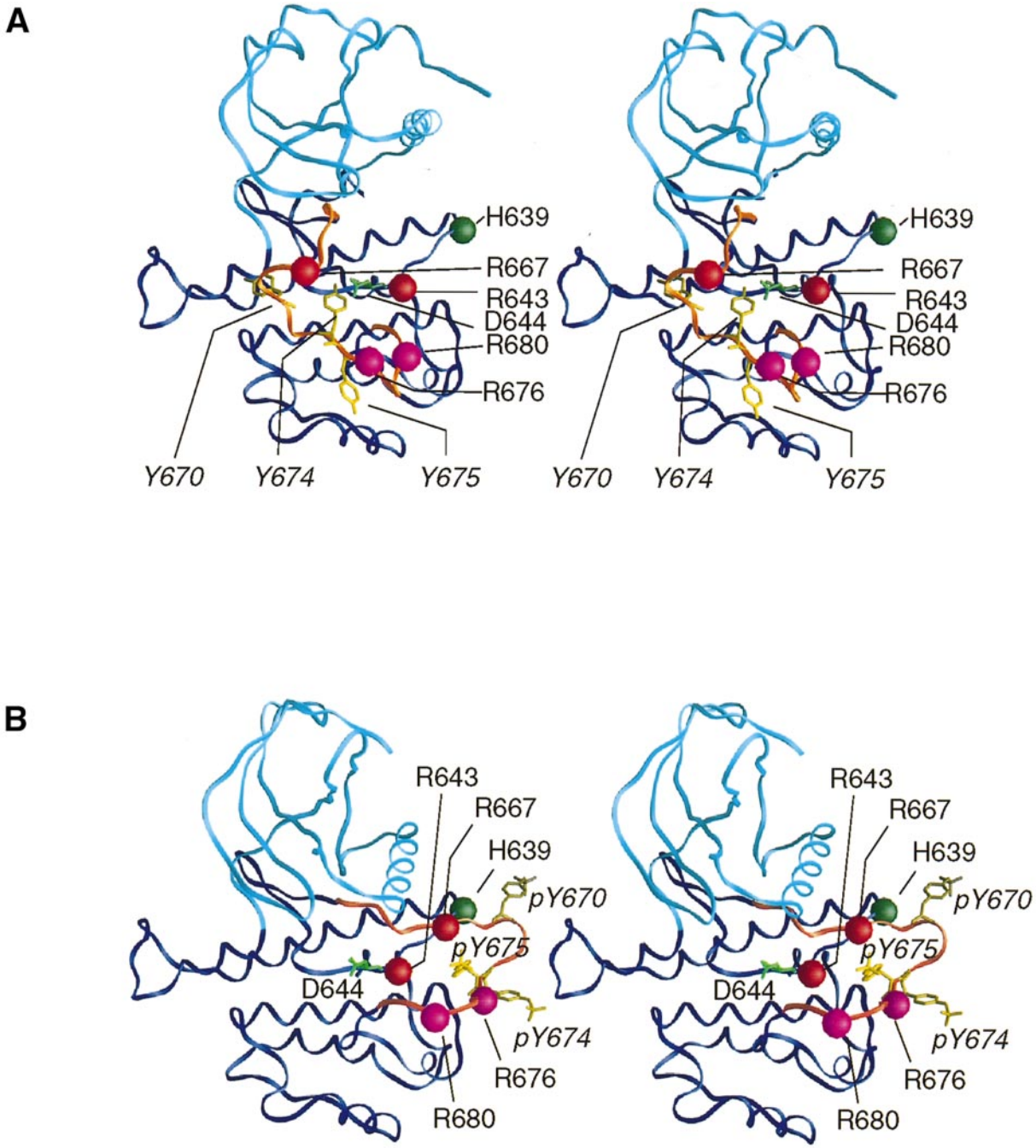

Fig. 7. Adapted structural model for the TRK activated state. Structural coordinates from the inactive (Brookhaven PDB, accession No. 1IRK) and activated (Brookhaven PDB, accession No. 1IR3) IRK crystal structures were adapted to depict graphically the TRK charge pair partners identified in this study. The N-terminal lobe of the kinase is colored light blue, the C-terminal lobe is dark blue, and the activation loop is orange. The activation loop tyrosines are colored yellow, the critical Asp644 is light green, and the interactors for pY670, pY674 and pY675 are colored dark green, magenta and red, respectively. With the exception of the activation loop, the C-terminal lobes of the structures are identically placed to aid in interpretation. (**A**) The inactive conformation of IRK, with homologous TRK residues identified, and (**B**) the active conformation. The stereo images were prepared using GRASP (Nicholls *et al*., 1991).

pY674) with Arg1164 (TRK Arg676) and of pY1163 (TRK pY675) with Arg1155 (TRK Arg667). There was no reported interactor for pY1158 (TRK Tyr670). Finally, although our findings point to Arg696 and Lys697 as functional contributors to stabilization of the TRK activation loop that do not interact with phosphotyrosines therein, equivalent basic residues are not present in IRK.

The above interactions indicate several points of interest. First, each of the activated structures (including that of TRK) includes interactions between residues homologous to TRK pY675 and Arg667; like TRK, PKA and LCK also show interactions corresponding to that of pY675 with Arg643. In contrast, the latter corresponding interaction was not reported for IRK. However, their proximity in the structure may permit these sites to interact during the activation process. The equivalent of Arg643 is conserved at the majority of sequenced serine/threonine and tyrosine kinases (Hanks *et al*., 1988; Hanks and Quinn,

1991), and hence this has the potential to be a widely utilized interacting partner for the functional homologs for pY675 (which are present in essentially all known protein kinases). Secondly, both TRK and activated IRK display interaction of residues homologous to TRK pY674 and Arg676, but no interaction with the homolog of TRK Arg680 (IRK Lys1168) was reported. Thirdly, in contrast to our observations for TRK pY670 and His639, no charge–charge interaction was reported for the corresponding phosphotyrosine (pY1158) and positively charged site (Lys1127 or Lys1126) in activated IRK. This may indicate a difference in placement between the two activation loops. It is of interest, however, that the majority of sequenced RTKs have a histidine, lysine or arginine residue at sites homologous to TRK 638 or 639 (Hanks *et al*., 1988; Hanks and Quinn, 1991) and either a Tyr670 equivalent or a nearby standing negative/polar charge (Martin-Zanca *et al*., 1986; Hanks and Quinn, 1991), so there is the possibility that this is also an interaction of general importance. Lastly, although TRK Arg696 and Lys697 have no homologs in IRK, one or two basic residues are present at the homologous sites in several RTKs including EGFR, NEU, c-Met, and RET as well as several Src family members (Hanks *et al*., 1988).

Our findings, coupled with structural information from IRK (Hubbard *et al*., 1994; Hubbard, 1997) and other kinases, suggest a physical model for disposition of the activation loop in activated TRK. When mapped onto the IRK structures (Figure 7), the TRK interactions identified in this study appear to be generally similar to those reported for IRK, suggesting that the two kinases have similar activation loop conformations. However, there are potential differences in their specific predicted conformations. The phosphorylated TRK activation loop is anchored by at least five associations that affect its localization. The associations between pY675 Arg643 and Arg667 appear to constrain the loop so that the nearby catalytic loop, and critical Asp644, is sterically unhindered. This appears to be accomplished in part by anchoring the middle portion of the activation loop to a contact that is outside of the catalytic core and outside of the activation loop itself (Arg643). However, this contact might still permit formation of a looping sub-segment (Asp668–Tyr674) within the overall activation loop that would probably retain mobility. The interactions of pY674 with Arg676 (and potentially Arg680), of pY670 with His639, and of pY675 with Arg667 would have the potential to limit this mobility and thus further minimize steric hindrance in the area of the catalytic core. Additionally, although not reported for activated IRK (Hubbard, 1997), the charge pair interactions of the activation loop may serve to orient the P + 1 loop of the kinase domain for proper substrate recognition as appears to be the case in the activated ERK2 crystal structure (Canagarajah *et al*., 1997). This mechanism of altered substrate recognition could account for the loss of phosphorylation of Tyr785, and consequently PLCγ-1, in the TRK activation loop tyrosine mutants (Cunningham *et al*., 1997). Finally, although the interactors for Arg696 and Lys697 are not identified presently, our functional studies permit the speculation that these residues also contribute to stabilizing the loop in a non-inhibitory conformation.

Clinical consequences of charge pair mutations in RTKs

Although mutational studies have established the importance of activation loop phosphotyrosines for RTK function, systematic structure–function studies of potential charge pair partners have not been presented previously. It is therefore of interest that several naturally occurring mutations support our findings. The naturally occurring R1152Q mutation in the human insulin receptor is associated with non-insulin-dependent diabetes mellitus (NIDDM) (Petruzziello *et al*., 1993). This residue corresponds to Arg1164 in the IRK structure, which interacts with IRK pY1162, and thus the mutation would be expected to have the functional consequences reported here for disrupting the Arg676–pY674 interaction in TRK. The naturally occurring insulin receptor R1131Q mutation is also associated with NIDDM (Kishimoto *et al*., 1994). Although no interactor for this site was reported in the activated IRK, our findings indicate that the homolog of this site in TRK (Arg643) interacts with an activation loop phosphotyrosine (TRK pY675/IRK pY1163). Thus, our observations suggest that the disease state associated with the insulin receptor R1131Q mutation is due to disruption of a charge pair normally formed by R1131 and pY1163. Another NIDDM-associated mutation of the insulin receptor activation loop is M1153I (Cama *et al*., 1991, 1992), which probably prevents proper acquisition of activation loop conformation due to the bulky nature of the substitution. An additional example involves the RET RTK. Here, mutation of Arg897 to glutamine leads to a Hirschsprung's disease-like state (Schuchardt *et al*., 1994). A similar phenotype is observed with a complete loss of RET, and so the mutation apparently compromises function (Romeo *et al*., 1994; Shimotake *et al*., 1997). RET Arg897 corresponds to TRK Arg667, which is a charge pair interactor for TRK pY675. Thus, our findings indicate that mutation of RET Arg897 compromises its interaction with an activation loop phosphotyrosine and thereby compromises receptor activity and function.

Materials and methods

Construction of TRK mutants, and production of LNC(TRK)s

The generation of *TRK* tyrosine to phenylalanine mutations was described previously (Cunningham *et al*., 1997). *TRK* mutants containing R643A and K541A in the Y674F and Y675F backgrounds were constructed using single-strand mutagenesis (Bio-Rad) as described previously (Stephens *et al*., 1994). The same mutations in the wild-type and Y670F backgrounds were generated by subcloning zonal mutations using restriction enzyme-generated cassettes. All other mutations of positively charged residues were generated using overlapping PCR (Higuchi, 1989) on each of the wild-type or single tyrosine mutant backgrounds, or by subcloning zonal cassettes onto these backgrounds. All mutant constructs were confirmed by sequencing. Mutant *TRKs* subsequently were cloned into the pLNC-X.5 retroviral expression vector using *Hin*dIII and *Xho*I, or through an additional TRK-internal *Bst*XI site. Retrovirus was produced by transient transfection of the constructs into Bosc 23 cells (Pear *et al*., 1993, 1996), and cellular supernatants from, or co-cultures of, these cells were used to infect NIH 3T3 and PC12nnr5 cells, respectively (described below; see also Cunningham *et al*., 1999). To confirm recombinant retrovirus construct integrity, TRK expression from each of the plasmids was evaluated by Western immunoblotting immunoprecipitates of TRK from stably transfected NIH 3T3 or PC12nnr5 cells, and/or total cell protein from Bosc 23 cells transiently transfected for 24–48 h.

Cell culture, retroviral infection and NGF treatment

NIH 3T3 subclone 'N' cells are a subpopulation of cells originally obtained from the ATCC and selected for flat morphology and low

apparent transformed phenotype (generously provided by Dr Gregg Gundersen, Columbia University, Department of Anatomy and Cell Biology). Cells were maintained on tissue culture plastic in high glucose Dulbecco's modified Eagle's medium (DMEM) supplemented with 10% heat-inactivated normal calf serum. Bosc 23 cells (Pear *et al*., 1993) (provided by Dr Jan Kitajewski, Columbia University, Department of Pathology) were maintained on tissue culture plastic in DMEM supplemented with 10% fetal bovine serum. PC12 cell derivatives were grown on collagen-coated tissue culture dishes as previously described (Greene and Tischler, 1976; Greene *et al*., 1998; Teng *et al*., 1998).

Retroviral infections were carried out by adding virus-containing supernatant recovered from packaging cell lines or through co-culture with mitomycin-treated Bosc 23 cells (Greene *et al*., 1998; Cunningham *et al*., 1999). Retroviral infection of 3T3-'N' cells was carried out by adding 1 ml of virus-containing Bosc 23 supernatant to nearly confluent monolayers maintained in 35 mm 6-well plates in 2–3 ml of growth medium. After 4–10 h, cells were subcultured into 10 cm plates and placed back in culture. After 24 h, cultures were either not treated or treated with 1 mg/ml G418 (Fisher), or 150 ng/ml NGF. Viral titers were determined by counting G418-resistant colonies for each of the infections. Co-culture of Bosc 23 cells with PC12nnr-5 cells was initiated after a 5 h mitomycin treatment (10 μg/ml final concentration) of Bosc 23 cells followed by extensive washing of treated Bosc 23 cells with growth medium. Co-cultures were maintained for 1 week prior to G418 selection, were selected for 2 weeks (500 μg/ml active) and were expanded as polyclonal/mass cultures.

NGF-induced TRK-dependent transformation of 3T3-'N' cells was assessed in cultures treated with NGF, or not, for up to 2 weeks. Transformed clusters of cells were quantified under low power using an inverted microscope. Transformation efficiency was derived by dividing the transformation quantification (the number of transformed clusters) by the viral titer (the number of G418-resistant colonies) and expressing the ratio as a percentage. NGF non-treated sister cultures were monitored to confirm that transformation was due to TRK ligand occupancy, and in no case were spontaneous transformation events detected that matched the above morphology. TRK immunostaining was achieved with anti-TRK (203) at a 1:200 dilution with fixed, attached cells (Harlow and Lane, 1988).

NGF-induced PC12nnr5 cell neuritogenesis rescue was assessed in cultures grown in RPMI 1640 medium supplemented with 1% heat-inactivated horse serum, as described previously (Greene and Tischler, 1976; Loeb *et al*., 1991). NGF-treated (100 ng/ml) and untreated cultures were scored for time periods of up to 1 week by determining the presence or absence of neurites on cells chosen at random ($n \geqslant 300$). Results reported are those of a representative, duplicate experiment, and error bars indicate ± SEM. Recombinant hNGF was a generous gift from Genetech Inc.

Immunoprecipitation and Western immunoblotting

NGF treatment of cultures was accomplished by addition of a small aliquot of concentrated stock to a final concentration of 100 ng/ml. After the indicated treatment time, cells were washed with ice-cold phosphate-buffered saline (PBS)/Tris-buffered saline (TBS), lysed in Triton-containing buffer, clarified by ultracentrifugation (100 000 *g* for 15 min at 4°C), normalized for protein content, and subjected to immunoprecipitation with the indicated antibodies, all as previously described (Loeb *et al*., 1992; Loeb and Greene, 1993). Immunoprobing was conducted with the indicated primary antibodies using the protocols and horseradish peroxidase-linked secondary antibodies of Amersham Life Science, followed by visualization by ECL (Amersham Corporation). Blots were reprobed with antibody after stripping in 2% SDS, 100 mM 2-mercaptoethanol and 62.5 mM Tris pH 6.8 and rocking at room temperature for ⩾16 h, or by placing blots into the same buffer pre-warmed to 50°C and shaking in a water bath for 45 min.

Acknowledgements

We thank Dr R.Stephens for providing the TRK R643A and K541A mutants in the Y674F and Y675F backgrounds, Drs M.Shelanski, S.Goff, W.Hendrickson and D.Kaplan for helpful discussions, Dr S.Hubbard for making the manuscript describing the IRK active structure available to us prior to publication, and Dr J.Williams for discussions and assistance in generating the structural models presented here. Support for this work was provided by grants from the National Institute of Neurological Disorders and Stroke (to L.A.G.), and Medical Scientist Training Program grant MSTP 5 T32 GM07367 (to M.E.C.)

References

Baron,V., Kaliman,P., Gautier,N. and Van Obberghen,E. (1992) The insulin receptor activation process involves localized conformational changes. *J. Biol. Chem.*, **267**, 23290–23294.

Bossemeyer,D. (1995) Protein kinases—structure and function. *FEBS Lett.*, **369**, 57–61.

Cama,A., De La Luz Sierra,M., Ottini,L., Kadowaki,T., Gorden,P., Imperato-McGinley,J. and Taylor,S.I. (1991) A mutation in the tyrosine kinase domain of the insulin receptor associated with insulin resistance in an obese woman. *J. Clin. Endocrinol. Metab.*, **73**, 894–901.

Cama,A., Quon,M.J., de la Luz Sierra,M. and Taylor,S.I. (1992) Substitution of isoleucine for methionine at position 1153 in the β-subunit of the human insulin receptor. *J. Biol. Chem.*, **267**, 8383–8389.

Canagarajah,B.J., Khokhlatchev,A., Cobb,M.H. and Goldsmith,E.J. (1997) Activation mechanism of the MAP kinase ERK2 by dual phosphorylation. *Cell*, **90**, 859–869.

Cordon-Cardo,C. *et al*. (1991) The *trk* tyrosine protein kinase mediates the mitogenic properties of nerve growth factor and neurotrophin-3. *Cell*, **66**, 173–183.

Cowley,S., Paterson,H., Kemp,P. and Marshall,C.J. (1994) Activation of MAP kinase kinase is necessary and sufficient for PC12 differentiation and for transformation of NIH 3T3 cells. *Cell*, **77**, 841–852.

Cunningham,M.E., Stephens,R.M., Kaplan,D.R. and Greene,L.A. (1997) Autophosphorylation of activation loop tyrosines regulates signaling by the TRK nerve growth factor receptor. *J. Biol. Chem.*, **272**, 10957–10967.

Cunningham,M.E., Kitajewski,J. and Greene,L.A. (1999) Efficient generation of stable pheochromocytoma (PC12) cell lines using a recombinant retrovirus (LNC). In Rush,R.A. (ed.), *Neurotrophin and Receptor Methods and Protocols*. Humana Press, Clifton, NJ, in press.

Evans,S.V. (1993) SETOR: hardware lighted three-dimensional solid model representations of macromolecules. *J. Mol. Graphics*, **11**, 134–138.

Green,S.H., Rydel,R.E., Connolly,J.L. and Greene,L.A. (1986) PC12 cell mutants that possess low- but not high-affinity nerve growth factor receptors neither respond to nor internalize nerve growth factor. *J. Cell Biol.*, **102**, 830–843.

Greene,L.A. (1984) The importance of both early and delayed responses in the biological responses of nerve growth factor. *Trends Neurosci.*, **7**, 91–94.

Greene,L.A. and Tischler,A.S. (1976) Establishment of a noradrenergic clonal line of rat adrenal pheochromocytoma cells which respond to nerve growth factor. *Proc. Natl Acad. Sci. USA*, **73**, 2424–2428.

Greene,L.A., Farinelli,S.E., Cunningham,M.E. and Park,D.S. (1998) Culture and experimental use of the PC12 rat pheochromocytoma cell line. In Banker,G. and Goslin,K. (eds), *Culturing Nerve Cells*. MIT Press, Cambridge, MA, pp. 161–188.

Hanks,S.K. and Quinn,A.M. (1991) Protein kinase catalytic domain sequence database: identification of conserved features of primary structure and classification of family members. *Methods Enzymol.*, **200**, 38–62.

Hanks,S.K., Quinn,A.M. and Hunter,T. (1988) The protein kinase family: conserved features and deduced phylogeny of the catalytic domains. *Science*, **241**, 42–52.

Harlow,E. and Lane,D. (1988) *Antibodies: A Laboratory Manual*. Cold Spring Harbor Laboratory Press, Cold Spring Harbor, NY.

Hernández-Sánchez,C., Blakesley,V., Kalebic,T., Helman,L. and LeRoith,D. (1995) The role of the tyrosine kinase domain of the insulin-like growth factor-I receptor in intracellular signaling, cellular proliferation and tumorigenesis. *J. Biol. Chem.*, **270**, 29176–29181.

Herrera,R. and Rosen,O.M. (1986) Autophosphorylation of the insulin receptor *in vitro*. *J. Biol. Chem.*, **261**, 11980–11985.

Higuchi,R. (1989) Using PCR to engineer DNA. In Erlich,H.A. (ed.), *PCR Technology—Principles and Applications for DNA Amplification*. Stockton Press, New York, NY, pp. 61–70.

Hubbard,S.R. (1997) Crystal structure of the activated insulin receptor tyrosine kinase in complex with peptide substrate and ATP analog. *EMBO J.*, **16**, 5572–5581.

Hubbard,S.R., Wei,L., Ellis,L. and Hendrickson,W.A. (1994) Crystal structure of the tyrosine kinase domain of the human insulin receptor. *Nature*, **372**, 746–754.

Johnson,L.N., Noble,M.E.M. and Owen,D.J. (1996) Active and inactive protein kinases: structural basis for regulation. *Cell*, **85**, 149–158.

Kaliman,P., Baron,V., Alengrin,F., Takata,Y., Webster,N.J.G., Olefsky,J.M. and Van Obberghen,E. (1993) The insulin receptor C-

terminus is involved in regulation of the receptor kinase activity. *Biochemistry*, **32**, 9539–9544.
Kishimoto,M., Hashiramoto,M., Yonezawa,K., Shii,K., Kazumi,T. and Kasuga,M. (1994) Substitution of glutamine for arginine 1131. A newly defined mutation in the insulin catalytic loop of the tyrosine kinase domain of the human insulin receptor. *J. Biol. Chem.*, **269**, 11349–11355.
Li,S., Ferber,A., Miura,M. and Baserga,R. (1994) Mitogenicity and transforming activity of the insulin-like growth factor-1 receptor with mutations in the tyrosine kinase domain. *J. Biol. Chem.*, **269**, 32558–32564.
Loeb,D.M. and Greene,L.A. (1993) Transfection with *trk* restores 'slow' NGF binding, efficient NGF uptake and multiple NGF responses to NGF-nonresponsive PC12 cell mutants. *J. Neurosci*., **13**, 2919–2929.
Loeb,D.M., Maragos,J., Martin-Zanca,D., Chao,M.V., Parada,L.F. and Greene,L.A. (1991) The *trk* proto-oncogene rescues NGF responsiveness in mutant NGF-nonresponsive PC12 cell lines. *Cell*, **66**, 961–966.
Loeb,D.M., Tsao,H., Cobb,M.H. and Greene,L.A. (1992) NGF and other growth factors induce an association between ERK1 and the NGF receptor, gp140^{prototrk}. *Neuron*, **9**, 1053–1065.
Loeb,D.M., Stephens,R.M., Copeland,T., Kaplan,D.R. and Greene,L.A. (1994) A Trk nerve growth factor (NGF) receptor point mutation affecting interaction with phospholipase C-γ1 abolishes NGF-promoted peripherin induction but not neurite outgrowth. *J. Biol. Chem.*, **269**, 8901–8910.
Longati,P., Bardelli,A., Ponzetto,C., Naldini,L. and Comoglio,P.M. (1994) Tyrosines$^{1234–1235}$ are critical for activation of the tyrosine kinase encoded by the Met proto-oncogene (HGF receptor). *Oncogene*, **9**, 49–57.
Martin-Zanca,D., Hughes,S.H. and Barbacid,M. (1986) A human oncogene formed by the fusion of truncated tropomyosin and a protein tyrosine kinase sequence. *Nature*, **319**, 743–748.
McCarty,J.H. and Feinstein,S.C. (1998) Activation loop tyrosines contribute varying roles to TrkB autophosphorylation and signal transduction. *Oncogene*, **16**, 1691–1700.
McDonald,N.Q., Murray-Rust,J. and Blundell,T.L. (1995) The first structure of a receptor tyrosine kinase domain: a further step in understanding the molecular basis of insulin action. *Structure*, **3**, 1–6.
Mohammadi,M., Schlessinger,J. and Hubbard,S.R. (1996) Structure of the FGF receptor tyrosine kinase domain reveals a novel autoinhibitory mechanism. *Cell*, **86**, 577–587.
Nicholls,A., Sharp,K.A. and Honig,B. (1991) Protein folding and association: insights from the interfacial and thermodynamic properties of hydrocarbons. *Proteins*, **11**, 281–296.
Pear,W.S., Nolan,G.P., Scott,M.L. and Baltimore,D. (1993) Production of high-titer helper-free retroviruses by transient transfection. *Proc. Natl Acad. Sci. USA*, **90**, 8392–8396.
Pear,W.S., Scott,M.L. and Nolan,G.P. (1996) Generation of high titre, helper-free retroviruses by transient transfection. In Robbins,P. (ed.), *Methods in Molecular Medicine: Gene Therapy Protocols*. Humana Press, Totowa, NJ, pp. 41–57.
Petruzziello,A., Formisano,P., Miele,C., Di Finizio,B., Riccardi,G., Ferrara,A., Beguinot,L. and Beguinot,F. (1993) Defective insulin action in fibroblasts from noninsulin-dependent diabetes mellitus patients with Gln1152 insulin receptor mutation. *J. Clin. Endocrinol. Metab.*, **77**, 409–412.
Romeo,G. *et al*. (1994) Point mutations affecting the tyrosine kinase domain of the *RET* proto-oncogene in Hirschsprung's disease. *Nature*, **367**, 377–378.
Rosen,O.M., Herrera,R., Olowe,Y., Petruzzelli,L.M. and Cobb,M.H. (1983) Phosphorylation activates the insulin receptor tyrosine protein kinase. *Proc. Natl Acad. Sci. USA*, **80**, 3237–3240.
Schlessinger,J. and Ullrich,A. (1992) Growth factor signaling by receptor tyrosine kinases. *Neuron*, **9**, 383–391.
Schuchardt,A., D'Agati,V., Larsson-Blomberg,L., Constantini,F. and Pachnis,V. (1994) Defects in the kidney and enteric nervous system of mice lacking the tyrosine kinase receptor Ret. *Nature*, **367**, 380–383.
Segal,R.A., Bhattacharyya,A., Rua,L.A., Alberta,J.A., Stephens,R.M., Kaplan,D.R. and Stiles,C.D. (1996) Differential utilization of Trk autophosphorylation sites. *J. Biol. Chem.*, **271**, 20175–20181.
Shimotake,T., Iwai,N., Inoue,K., Kimura,T., Ichikawa,D., Abe,T. and Inazawa,J. (1997) Germline mutation of the *RET* proto-oncogene, in children with total intestinal aganglionosis. *J. Pediatr. Surg*., **32**, 498–500.
Stephens,R.M., Loeb,D.M., Copeland,T.D., Pawson,T., Greene,L.A. and Kaplan,D.R. (1994) Trk receptors use redundant signal transduction pathways involving SHC and PLCγ-1 to mediate neuritogenesis. *Neuron*, **12**, 1–20.
Teng,K.K., Angelastro,J.M., Cunningham,M.E., Farinelli,S.E. and Greene,L.A. (1998) Cultured PC12 cells: a model for neuronal function, differentiation and survival. In Celis,J.E. (ed.), *Cell Biology: A Laboratory Handbook*. 2nd edn. Academic Press, Orlando, FL, pp. 244–250.
Tornqvist,H.E. and Avruch,J. (1988) Relationship of site-specific β subunit tyrosine autophosphorylation to insulin activation of the insulin receptor (tyrosine) protein kinase activity. *J. Biol. Chem.*, **263**, 4593–4601.
Ullrich,A. and Schlessinger,J. (1990) Signal transduction by receptors with tyrosine kinase activity. *Cell*, **61**, 203–212.
Van Obberghen,E., Baron,V., Scimeca,J.-C. and Kaliman,P. (1993) Insulin receptor: receptor activation and signal transduction. *Adv. Second Messenger Phosphoprotein Res*., **28**, 195–201.
Wei,L., Hubbard,S.R., Smith,R.F. and Ellis,L. (1994) Protein kinase superfamily—comparisons of sequence data with three-dimensional structures. *Curr. Opin. Struct. Biol*., **4**, 450–455.
White,M.F., Shoelson,S.E., Keutmann,H. and Kahn,C.R. (1988) A cascade of tyrosine autophosphorylation in the β-subunit activates the phosphotransferase of the insulin receptor. *J. Biol. Chem.*, **263**, 2969–2980.
Yamaguchi,H. and Hendrickson,W.A. (1996) Structural basis for activation of human lymphocyte kinase Lck upon tyrosine phosphorylation. *Nature*, **384**, 484–489.
Zheng,J., Trafny,E.A., Knighton,D.R., Xuong,N.H., Taylor,S.S., Ten Eyck,L.F. and Sowadski,J.M. (1993) 2.2 Å refined crystal structure of the catalytic subunit of cAMP-dependent protein kinase complexed with MnATP and a peptide inhibitor. *Acta Crystallogr*., **D49**, 362–365.

Received September 14, 1998; revised October 21, 1998; accepted October 23, 1998